Deep Ordinal Regression Forests

Haiping Zhu, Yuheng Zhang, Hongming Shan, *Member*, Lingfu Che, Xiaoyang Xu, Junping Zhang, *Member*, Jianbo Shi, *Senior Member*, Fei-Yue Wang, *IEEE Fellow*

Abstract—Ordinal regression is a type of regression techniques used for predicting an ordinal variable. Recent methods formulate an ordinal regression problem as a series of binary classification problems. Such methods cannot ensure the global ordinal relationship is preserved since the relationships among different binary classifiers are neglected. We propose a novel ordinal regression approach called Deep Ordinal Regression Forests (DORFs), which is constructed with the differentiable decision trees for obtaining precise and stable global ordinal relationships. The advantages of the proposed DORFs are twofold. First, instead of learning a series of binary classifiers independently, the proposed method learns an ordinal distribution for ordinal regression. Second, the differentiable decision trees can be trained together with the ordinal distribution in an end-to-end manner. The effectiveness of the proposed DORFs is verified on two ordinal regression tasks, i.e., facial age estimation and image aesthetic assessment, showing significant improvements and better stability over the state-of-the-art ordinal regression methods.

Index Terms—Ordinal regression, differentiable decision trees, random forest, ordinal distribution learning.

I. INTRODUCTION

Ordinal regression has broad applications in real-world problems such as medical research [1]–[5], credit rating [6]–[9], age estimation [10], [11], image aesthetic assessment [12], [13], text classification [14] and more. As an intermediate problem between classification and regression, ordinal regression is used for predicting an ordinal variable [15], [16]. Imagining a situation where a doctor is asked to make an assessment of the severity of a patient's illness. The assessment scale can be {very healthy, healthy, slightly sick, sick, serious illness}. This is not a simple classification task, because his answer is not a clear right or wrong answer. But

Manuscript received xxx xx, 2020; revised xxx xx, 2020.

Haiping Zhu, Yuheng Zhang, Lingfu Che and Xiaoyang Xu are with the Shanghai Key Laboratory of Intelligent Information Processing, School of Computer Science, Fudan University, Shanghai, 200433, P.R. China, Email: {hpzhu14, yuhengzhang16, lfche16, xuxy17}@fudan.edu.cn

Hongming Shan is with the Shanghai Key Laboratory of Intelligent Information Processing, School of Computer Science, Fudan University, Shanghai, 200433, P.R. China, and with the Department of Biomedical Engineering, Jonsson Engineering Center, Rensselaer Polytechnic Institute, Troy, NY, 12180 USA, Email: shanh@rpi.edu

Junping Zhang is with the Shanghai Key Laboratory of Intelligent Information Processing, School of Computer Science, Fudan University, Shanghai, 200433, P.R. China; Tel.: +86-21-55664503, Fax: +86-21-65654253, Email: jpzhang@fudan.edu.cn

Jianbo Shi is with the GRASP Laboratory, University of Pennsylvania, Philadelphia, PA.; Email: jshi@seas.upenn.edu

Fei-Yue Wang is with the State Key Laboratory for Management and Control of Complex Systems, Institute of Automation, Chinese Academy of Sciences, Beijing 100190, China, and also with the Institute of Systems Engineering, Macau University of Science and Technology, Macau 999078, China, and also with the University of Chinese Academy of Sciences, Beijing 100049, China; Email: feiyue@ieee.org

Corresponding author: Junping Zhang and Fei-Yue Wang

it is also not a continuous regression task, because we only care about the discrete sorting between different diseases.

To solve the ordinal regression problem, traditional methods formulate it as a classification problem, which can be solved by many well-studied classification algorithms [17]–[22]. However, the ordinal information that can improve predictive performance is not used. Recent methods formulate it as a series of binary classifiers to model ordinal relationship [10], [11], [23]–[25] — each binary classifier recognizes a sample into two classes by judging whether its label is less than a specified class attribute. With more attention given to the ordinal information, these binary classification methods lead to better predictive performance. However, these methods learn a series of binary classifiers independently, thus the underlying global relationship among these binary classifiers is neglected. An example of such a deficiency is shown in Fig. 1 (b), where the output probability should be a decreasing trend, rather than increasing sometimes.

To overcome this deficiency of lack of global ordinal relationships, we present a Deep Ordinal Regression Forests (DORFs) approach. Our method utilizes the differentiable decision trees [26] to preserve the ordinal relationship by learning an ordinal distribution rather than learning a series of binary classifiers independently. There are three advantages of using the differentiable decision tree to handle the ordinal regression tasks. One is that the decision tree has the expressive power to model any ordinal distribution through a mixture of leaf node predictions. The second is the parameters of the split nodes in the differentiable decision tree can be learned in a back-propagation manner, which realizes the end-to-end combination of tree learning and presentation learning. The third is that the ensemble property of decision forests can alleviate the over-fitting issue. We regard the output of a decision tree as an ordinal distribution, followed by optimizing the DORFs by using the cross-entropy loss between the predicted and ground-truth ordinal distribution. We optimize the tree by iteratively updating split nodes and leaf nodes. Following [27], we optimize the leaf node predictions by Variational Boundary [28], [29] after fixing the split node, in which the loss function is replaced by its upper bound and then optimized by a discrete iterative function. To learn a forest, we use the averaged losses of all individual trees to optimize the forest, allowing the split nodes of different trees to be connected to the same output units of the feature learning function. Thus, the split node parameters of all individual trees can be learned jointly.

The contributions described in this paper are:

 We present a deep ordinal regression forests (DORFs) approach to solve the ordinal regression problem, in which the ordinal relationship can be well preserved.

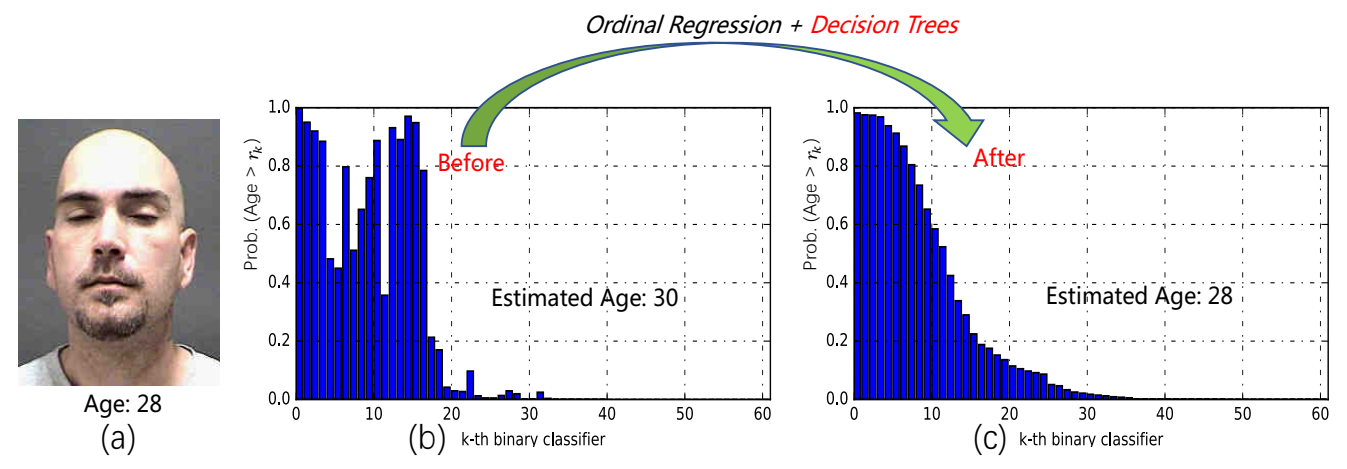


Fig. 1. Ordinal regression on the facial age estimation. Each k-th classifier computes the probability of the persons age is $> r_k$, where $r_k = r_1 + k - 1$ and $r_1 = 16$. The cross point of probability > 0.5 determines the persons age. (a) Current methods fail to preserve the global ordering of the ordinal distribution. (b) The DORFs produces ordinal distribution with well preserved global relationships.

This is the first work to obtain ordering results for ordinal regression with the differentiable decision tree.

- 2) We provide a theoretical derivation for the update rule of the leaf node.
- Experimental results demonstrate the effectiveness and the stability of our DORFs in modeling the ordinal distribution based on facial age estimation and image aesthetic assessment.

The rest of this paper is organized as follows. We first briefly recall the development of the random forests methods and the ordinal regression methods in Sec. II. And we then describe the detail of the proposed method in Sec. III. Finally, we analyze our experimental results in Sec. IV and give our conclusion in Sec. V.

II. RELATED WORK

Since the DORFs extends the differentiable decision trees to ordinal regression problems, we will briefly survey the development of random forests and ordinal regression in this section.

Random Forests are an ensemble of decision trees [30]-[33], each of which consists of several split nodes and leaf nodes. Meanwhile, the tree growing usually employs greedy algorithms to achieve a hard partition decision for each split node [30], which is intractable to integrate decision trees and representation learning in an end-to-end manner. Some hierarchical mixture of expert approaches [34], [35] can also be considered as tree-structured models, however, lacking both, representation learning and ensemble aspects. To address this issue, deep neural decision forests (dNDFs) [26] define a soft differentiable decision function at each split node to ensure that the parameters of the split nodes can be learned by back-propagation and utilize a global loss function on the tree to ensure the prediction of the leaf nodes can be updated by a discrete iterative function. Further, Shen et al. [27], [36] also extended this differentiable decision tree to solve the problems of label distribution learning. Similarly, the neural regression forest (NRF) [37] is proposed to use a tree of CNNs to jointly

learn the feature representation and decision functions for each node in the tree.

Ordinal Regression aims to learn a rule to predict ordinal labels. Traditional ordinal regression algorithms are modified from well-known classification methods [16]–[20], [38]–[41]. For instances, Herbrich et al. [16] utilized support vector machine (SVM) for ordinal regression, and then Shashua et al. [17] refined SVM to handle multiple thresholds. Crammer et al. [18] proposed the perceptron ranking algorithm to generalize the online perceptron algorithm with multiple thresholds for ordinal regression. Lin et al. [20] proposed a thresholded ensemble model for ordinal regression problems, which consists of a weighted ensemble of confidence functions and an ordered vector of thresholds. However, these methods formulate the ordinal regression as a classification task, ignoring the potential of ordinal information in improving predictive performance. Recently, some methods formulate the ordinal regression as a series of binary classifications [10], [11], [23]-[25], [42]. For examples, Frank et al. [23] utilized decision trees as binary classifiers for ordinal regression. Li et al. [42] proposed a framework to reduce an ordinal regression problem as a set of classification problems, and employed an SVM to solve the classification problems. Niu et al. [10] introduced a CNN network with multiple binary outputs to solve the ordinal regression for age estimation. Chen et al. [11] proposed to learn multiple binary CNNs, and then aggregated the final outputs. With more attention given to the ordinal information, these binary classification methods lead to better predictive performance. However, these methods learn each binary classifier separately and independently, ignoring the global ordinal relationship among these binary classifiers. To better preserve the ordinal relationship among these binary classifiers, in this paper, we propose a novel ordinal regression method by extending the differentiable decision trees to deal with the ordinal regression problems.

III. DEEP ORDINAL REGRESSION FORESTS

In this section, we first introduce the formulation of DORFs and then describe how to learn a single decision tree with or-

dinal regression. Finally, we formulate the learning procedure of the decision forests, which are an ensemble of decision trees.

A. Ordinal Regression

Let $\mathcal X$ be the input space and $\mathcal Y=\{r_1,r_2,\cdots,r_K\}$ be the label space with ordered ranks $r_1\preceq r_2\preceq \cdots \preceq r_K$, where K is the number of possible label ranks and the symbol \preceq denotes the order among different ranks. The ordinal regression is to learn a mapping function $h:\mathcal X\to\mathcal Y$. Following recent studies [10], [11], [23], [25], we decompose the original ordinal regression with K ranks into K-1 binary classification tasks. For each rank r_k , a binary classifier g_k is built to classify a sample $x\in\mathcal X$ into two classes and the ground-truth label of the sample x depends on whether label $y\in\mathcal Y$ is greater than r_k . The label of x in classifier y is 1 if $y>r_k$ and 0 otherwise. Note that the output of y is a value between 0 and 1. Thus, the final rank of a sample x can be predicted as

$$h(\mathbf{x}) = r_1 + \eta \sum_{k=1}^{K-1} \mathbf{1} [g_k(\mathbf{x}) > 0.5],$$
 (1)

where η is the partitioning interval, $\mathbf{1}[\cdot]$ denotes a truth-test indicator function, which is 1 if the inner condition holds, and 0 otherwise. Let $\mathcal{D} \in \mathbb{R}^{(K-1)\times 1}$ denote an ordinal distribution label space, we can transform the label y as an ordinal distribution label $d=(d^1,d^2,\cdots,d^{K-1})^T\in\mathcal{D}$, where $d^k=1$ if $y>r_k$; otherwise $d^k=0$. Therefore, the goal of an ordinal regression problem is instead to learn a mapping function $g:\mathcal{X}\to\mathcal{D}$, where the binary classifier g_k is the k-th element in g.

B. Decision Tree with Ordinal Distribution

According to the definition of the ordinal regression, our goal becomes to learn a mapping function g through a decision tree based structure \mathcal{T} . Each decision tree consists of a set of split nodes \mathcal{N} and a set of leaf nodes \mathcal{L} . Specifically, we define a decision function $s_n(\cdot; \Theta) : \mathcal{X} \to \{0,1\}$ on each split node, parameterized by Θ to determine which node (left or right) a sample can be assigned to. And we assume that each leaf node $l \in \mathcal{L}$ holds an ordinal distribution $\pi_l = (\pi_l^1, \pi_l^2, \cdots, \pi_l^{K-1})^T$ over \mathcal{D} . Following [26], [36], we also use the decision function $s_n(x; \Theta) = \sigma(f_{\varphi(n)}(x; \Theta))$ to build a differentiable decision tree. Each decision function $\sigma(\cdot)$ is set as a sigmoid function and the $\varphi(\cdot)$ is an index function that maps the $\varphi(n)$ -th output of function $f(x; \Theta)$ on the corresponding split node n. Let d denote the dimension of the feature function output, then $f: x o \mathbb{R}^d$ is a real-valued feature learning function, depending on the sample x and the parameter Θ . In principle, the function f can be any function. In this paper, we use a deep neural networks as the feature function f, which is learned in an end-to-end manner. The indexed function $\varphi(\cdot)$ between the split nodes and the output units of function f is initialized randomly before the tree learning. An example shown in Fig. 2 demonstrates how to construct a decision forest based on $\varphi(\cdot)$. Then, the probability

of a sample x falling into leaf node l is given by

$$p(l|\boldsymbol{x};\boldsymbol{\Theta}) = \prod_{n \in \mathcal{N}} s_n(\boldsymbol{x};\boldsymbol{\Theta})^{\mathbf{1}[l \in \mathcal{L}_n^l]} (1 - s_n(\boldsymbol{x};\boldsymbol{\Theta}))^{\mathbf{1}[l \in \mathcal{L}_n^r]}, (2)$$

where $\mathbf{1}[\cdot]$ is an indicator function, and \mathcal{L}_n^l and \mathcal{L}_n^r denote the sets of leaf nodes held by the left and right subtrees of node n, \mathcal{T}_n^l and \mathcal{T}_n^r , respectively. Therefore, given a sample \boldsymbol{x} , the mapping function \boldsymbol{g} , based on the decision tree \mathcal{T} , is defined by

$$g(x; \Theta, T) = \sum_{l \in L} p(l|x; \Theta) \pi_l.$$
 (3)

C. Tree Optimization

Given a training set $S = \{(\boldsymbol{x}_i, \boldsymbol{d}_i)\}_{i=1}^N$, our goal is to learn a decision tree \mathcal{T} described in III-A, which can output an ordinal distribution $\boldsymbol{g}(\boldsymbol{x}_i; \boldsymbol{\Theta}, \mathcal{T})$ in reference to \boldsymbol{d}_i for each sample \boldsymbol{x}_i . A straightforward way is to minimize the cross entropy loss between each $\boldsymbol{g}(\boldsymbol{x}_i; \boldsymbol{\Theta}, \mathcal{T})$ and \boldsymbol{d}_i ,

$$\mathcal{R}(\boldsymbol{\pi}, \boldsymbol{\Theta}; \mathcal{S}) = -\frac{1}{N} \sum_{i=1}^{N} \sum_{k=1}^{K-1} \left(d_i^k \log \left(g_k(\boldsymbol{x}_i; \boldsymbol{\Theta}, \mathcal{T}) \right) + (1 - d_i^k) \log \left(1 - g_k(\boldsymbol{x}_i; \boldsymbol{\Theta}, \mathcal{T}) \right) \right)$$

$$= -\frac{1}{N} \sum_{i=1}^{N} \sum_{k=1}^{K-1} \left(d_i^k \log \left(\sum_{l \in \mathcal{L}} p(l|\boldsymbol{x}_i; \boldsymbol{\Theta}) \pi_l^k \right) + (1 - d_i^k) \log \left(1 - \sum_{l \in \mathcal{L}} p(l|\boldsymbol{x}_i; \boldsymbol{\Theta}) \pi_l^k \right) \right),$$

$$= -\frac{1}{N} \sum_{i=1}^{N} \sum_{k=1}^{K-1} \left(d_i^k \log \left(\sum_{l \in \mathcal{L}} p(l|\boldsymbol{x}_i; \boldsymbol{\Theta}) \pi_l^k \right) + (1 - d_i^k) \log \left(\sum_{l \in \mathcal{L}} p(l|\boldsymbol{x}_i; \boldsymbol{\Theta}) (1 - \pi_l^k) \right) \right), \quad (4)$$

where π denotes the ordinal distributions held by all the leaf nodes \mathcal{L} and $g_k(\boldsymbol{x}_i; \boldsymbol{\Theta}, \mathcal{T})$ is the k-th output unit of $g(\boldsymbol{x}_i; \boldsymbol{\Theta}, \mathcal{T})$. For the simplicity of the math expression, we use $d_i^{(k,c=1)}$ and $d_i^{(k,c=2)}$ to denote d_i^k and $(1-d_i^k)$, respectively. Correspondingly, $\pi_l^{(k,c=1)}$ and $\pi_l^{(k,c=2)}$ denote π_l^k and $(1-\pi_l^k)$. Thus the objective function Eq. (4) is simplified as:

$$= -\frac{1}{N} \sum_{i=1}^{N} \sum_{k=1}^{K-1} \sum_{c=1}^{2} \left(d_{i}^{(k,c)} \log(\sum_{l \in \mathcal{L}} p(l | \boldsymbol{x}_{i}; \boldsymbol{\Theta}) \pi_{l}^{(k,c)}) \right)$$
s.t. $\forall l, k, \sum_{i=1}^{2} \pi_{l}^{(k,c)} = 1,$ (5)

where we have $\sum_{c=1}^{2} d_i^{(k,c)} = 1$ for $\forall k$. Note that learning a tree \mathcal{T} requires to estimate the parameters Θ of the split nodes and the ordinal distributions π of the leaf nodes. The optimal parameters (Θ^*, π^*) are determined by

$$(\mathbf{\Theta}^{\star}, \boldsymbol{\pi}^{\star}) = \arg\min_{\mathbf{\Theta}, \boldsymbol{\pi}} \mathcal{R}(\boldsymbol{\pi}, \mathbf{\Theta}; \mathcal{S}).$$
 (6)

We solve Eq. (6) through an alternative optimization strategy, that is, optimizing π and Θ alternatively.

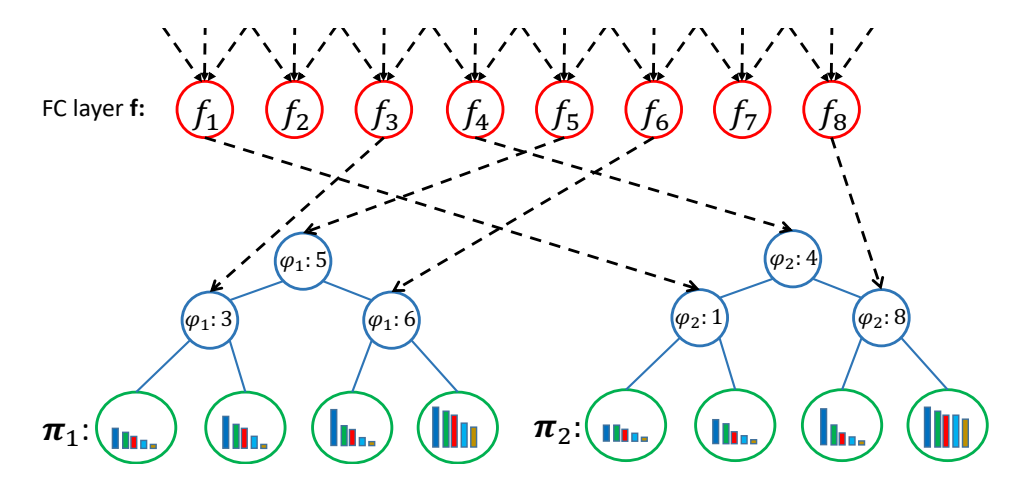


Fig. 2. The tree structure of our DORFs. The red circles at the top represent the output units of the function f parameterized by Θ , which can be a feature vector or a fully-connected (FC) layer of a deep neural network. The blue and green circles are split nodes and leaf nodes, respectively. Two index functions φ_1 and φ_2 are assigned to these two trees respectively. The black dashed arrows indicate the correspondence between the split nodes of the two trees and the output units of the FC layer. Each tree has independent leaf node ordinal distribution, and the final output of a forest is the average output of all the individual trees.

D. Learning Split Nodes

Next, we describe how to update the parameters Θ for split nodes, when the ordinal distribution held by the leaf nodes π is fixed. The gradient of the loss $\mathcal{R}(\pi,\Theta;\mathcal{S})$ with respect to Θ can be computed by the following chain rule:

$$\frac{\partial \mathcal{R}(\boldsymbol{\pi}, \boldsymbol{\Theta}; \mathcal{S})}{\partial \boldsymbol{\Theta}} = \sum_{i=1}^{N} \sum_{n \in \mathcal{N}} \frac{\partial \mathcal{R}(\boldsymbol{\pi}, \boldsymbol{\Theta}; \mathcal{S})}{\partial f_{\varphi(n)}(\boldsymbol{x}_i; \boldsymbol{\Theta})} \frac{\partial f_{\varphi(n)}(\boldsymbol{x}_i; \boldsymbol{\Theta})}{\partial \boldsymbol{\Theta}},$$
(7)

where only the first term depends on the tree and the second term depends on the specific type of the function $f_{\varphi(n)}$.

Given the definitions for our decision functions $s_n(x; \Theta)$ and the log-loss $\mathcal{R}(\pi, \Theta; \mathcal{S})$, we can derive the first gradient term in Eq. (7) as follows:

$$\frac{\partial \mathcal{R}(\boldsymbol{\pi}, \boldsymbol{\Theta}; \mathcal{S})}{\partial f_{\varphi(n)}(\boldsymbol{x}_i; \boldsymbol{\Theta})} = \sum_{l \in \mathcal{L}} \frac{\partial \mathcal{R}(\boldsymbol{\pi}, \boldsymbol{\Theta}; \mathcal{S})}{\partial p(l|\boldsymbol{x}_i; \boldsymbol{\Theta})} \frac{\partial p(l|\boldsymbol{x}_i; \boldsymbol{\Theta})}{\partial f_{\varphi(n)}(\boldsymbol{x}_i; \boldsymbol{\Theta})}$$

$$= -\frac{1}{N} \sum_{k=1}^{K-1} \sum_{c=1}^{2} \sum_{l \in \mathcal{L}} \frac{d_i^{(k,c)} \pi_l^{(k,c)}}{\sum_{l \in \mathcal{L}} (p(l|\boldsymbol{x}_i; \boldsymbol{\Theta}) \pi_l^{(k,c)})} \frac{\partial p(l|\boldsymbol{x}_i; \boldsymbol{\Theta})}{\partial f_{\varphi(n)}(\boldsymbol{x}_i; \boldsymbol{\Theta})}$$

$$= -\frac{1}{N} \sum_{k=1}^{K-1} \sum_{c=1}^{2} \sum_{l \in \mathcal{L}} \frac{d_i^{(k,c)} \pi_{l(k,c)} p(l|\boldsymbol{x}_i; \boldsymbol{\Theta})}{\sum_{l \in \mathcal{L}} (p(l|\boldsymbol{x}_i; \boldsymbol{\Theta}) \pi_{l(k,c)})} \frac{\partial \log p(l|\boldsymbol{x}_i; \boldsymbol{\Theta})}{\partial f_{\varphi(n)}(\boldsymbol{x}_i; \boldsymbol{\Theta})}.$$
(8)

Here $p(l|\boldsymbol{x};\boldsymbol{\Theta}) = \prod_{n \in \mathcal{N}} s_n(\boldsymbol{x};\boldsymbol{\Theta})^{\mathbf{1}[l \in \mathcal{L}_n^l]} (1 - s_n(\boldsymbol{x};\boldsymbol{\Theta}))^{\mathbf{1}[l \in \mathcal{L}_n^r]}$, and $s_n(\boldsymbol{x};\boldsymbol{\Theta}) = \sigma(f_{\varphi(n)}(\boldsymbol{x};\boldsymbol{\Theta}))$. Thus, we have

$$\frac{\partial \log p(l|\mathbf{x}_i; \mathbf{\Theta})}{\partial f_{\varphi(n)}(\mathbf{x}_i; \mathbf{\Theta})} = \frac{\partial \log s_n(\mathbf{x}_i; \mathbf{\Theta})^{\mathbf{1}[l \in \mathcal{L}_n^l]}}{\partial f_{\varphi(n)}(\mathbf{x}_i; \mathbf{\Theta})} + \frac{\partial \log(1 - s_n(\mathbf{x}_i; \mathbf{\Theta})^{\mathbf{1}[l \in \mathcal{L}_n^r]})}{\partial f_{\varphi(n)}(\mathbf{x}_i; \mathbf{\Theta})} = (1 - s_n(\mathbf{x}_i; \mathbf{\Theta})^{\mathbf{1}[l \in \mathcal{L}_n^l]}) - s_n(\mathbf{x}_i; \mathbf{\Theta})^{\mathbf{1}[l \in \mathcal{L}_n^r]}. \tag{9}$$

By substituting Eq. (9) to Eq. (8), we get $\frac{\partial \mathcal{R}(\boldsymbol{\pi}, \boldsymbol{\Theta}; \mathcal{S})}{\partial f_{\varphi(n)}(\boldsymbol{x}_{i}; \boldsymbol{\Theta})}$ $= \frac{1}{N} \sum_{k=1}^{K-1} \sum_{c=1}^{2} d_{i}^{(k,c)} \left(\frac{\sum_{l \in \mathcal{L}} p(l|\boldsymbol{x}_{i}; \boldsymbol{\Theta}) \pi_{l}^{(k,c)} s_{n}(\boldsymbol{x}_{i}; \boldsymbol{\Theta})^{\mathbf{1}[l \in \mathcal{L}_{n}^{r}]}}{\sum_{l \in \mathcal{L}} (p(l|\boldsymbol{x}_{i}; \boldsymbol{\Theta}) \pi_{l}^{(k,c)})} \right)$ $\frac{\sum_{l \in \mathcal{L}} p(l|\boldsymbol{x}_{i}; \boldsymbol{\Theta}) \pi_{l}^{(k,c)} (1 - s_{n}(\boldsymbol{x}_{i}; \boldsymbol{\Theta})^{\mathbf{1}[l \in \mathcal{L}_{n}^{l}]})}{\sum_{l \in \mathcal{L}} (p(l|\boldsymbol{x}_{i}; \boldsymbol{\Theta}) \pi_{l}^{(k,c)})} \right)$ $= \frac{1}{N} \sum_{k=1}^{K-1} \sum_{c=1}^{2} d_{i}^{(k,c)} \left(s_{n}(\boldsymbol{x}; \boldsymbol{\Theta}) \frac{\sum_{l \in \mathcal{L}^{r}} p(l|\boldsymbol{x}_{i}; \boldsymbol{\Theta}) \pi_{l}^{(k,c)}}{\sum_{l \in \mathcal{L}} (p(l|\boldsymbol{x}_{i}; \boldsymbol{\Theta}) \pi_{l}^{(k,c)})} \right)$ $(1 - s_{n}(\boldsymbol{x}; \boldsymbol{\Theta})) \frac{\sum_{l \in \mathcal{L}^{l}} p(l|\boldsymbol{x}_{i}; \boldsymbol{\Theta}) \pi_{l}^{(k,c)}}{\sum_{l \in \mathcal{L}} (p(l|\boldsymbol{x}_{i}; \boldsymbol{\Theta}) \pi_{l}^{(k,c)})} \right)$ $= \frac{1}{N} \sum_{k=1}^{K-1} \sum_{c=1}^{2} d_{i}^{(k,c)} \left(s_{n}(\boldsymbol{x}; \boldsymbol{\Theta}) \frac{g_{(k,c)}(\boldsymbol{x}_{i}; \boldsymbol{\Theta}, \mathcal{T}^{r})}{g_{(k,c)}(\boldsymbol{x}_{i}; \boldsymbol{\Theta}, \mathcal{T})} - (1 - s_{n}(\boldsymbol{x}; \boldsymbol{\Theta})) \frac{g_{(k,c)}(\boldsymbol{x}_{i}; \boldsymbol{\Theta}, \mathcal{T}^{l})}{g_{(k,c)}(\boldsymbol{x}_{i}; \boldsymbol{\Theta}, \mathcal{T})} \right), \tag{10}$

where $g_{(k,c)}(\boldsymbol{x}_i;\boldsymbol{\Theta},\mathcal{T}^l) = \sum_{l\in\mathcal{L}^l} p(l|\boldsymbol{x}_i;\boldsymbol{\Theta}) \pi_l^{(k,c)}$ and $g_{(k,c)}(\boldsymbol{x}_i;\boldsymbol{\Theta},\mathcal{T}) = \sum_{l\in\mathcal{L}} p(l|\boldsymbol{x}_i;\boldsymbol{\Theta}) \pi_l^{(k,c)}$. Note that, we have $g_{(k,c)}(\boldsymbol{x}_i;\boldsymbol{\Theta},\mathcal{T}) = g_{(k,c)}(\boldsymbol{x}_i;\boldsymbol{\Theta},\mathcal{T}^l) + g_{(k,c)}(\boldsymbol{x}_i;\boldsymbol{\Theta},\mathcal{T}^r)$, which indicates that the gradient computation in **Eq.** (10) can be started at the leaf nodes and carried out in a bottom-up manner. Thus, the parameters of split node can be learned by standard back-propagation.

E. Learning Leaf Nodes

Given the updating rules for the decision function parameters Θ from the previous subsection, we now consider the constrained convex optimization problem of minimizing Eq. (5) with respect to π when Θ is fixed, *i.e.*

$$\min_{\boldsymbol{\pi}} \mathcal{R}(\boldsymbol{\pi}, \boldsymbol{\Theta}; \mathcal{S}), \quad \boldsymbol{s.t.} \quad \forall \ l, k, \ \sum_{c=1}^{2} \pi_{l}^{(k,c)} = 1.$$
 (11)

One possible way to address this constrained optimization problem is to use *variational bounding* [28], [29], which leads to a step-size free and fast-converged update rule for π . Similar to [36], an upper bound for the loss function $\mathcal{R}(\pi,\Theta;\mathcal{S})$ can be obtained by Jensen's inequality:

$$\begin{split} &\mathcal{R}(\boldsymbol{\pi},\boldsymbol{\Theta};\mathcal{S}) \\ &= -\frac{1}{N} \sum_{i=1}^{N} \sum_{k=1}^{K-1} \sum_{c=1}^{2} d_{i}^{(k,c)} \log \left(\sum_{l \in \mathcal{L}} p(l|\boldsymbol{x}_{i};\boldsymbol{\Theta}) \pi_{l}^{(k,c)} \right) \\ &\leq -\frac{1}{N} \sum_{i=1}^{N} \sum_{k=1}^{K-1} \sum_{c=1}^{2} d_{i}^{(k,c)} \sum_{l \in \mathcal{L}} \xi_{l}(\bar{\pi}_{l}^{(k,c)},\boldsymbol{x}_{i}) \log \left(\frac{p(l|\boldsymbol{x}_{i};\boldsymbol{\Theta}) \pi_{l}^{(k,c)}}{\xi_{l}(\bar{\pi}_{l}^{(k,c)},\boldsymbol{x}_{i})} \right), \\ &\text{where } \xi_{l}(\boldsymbol{\pi}_{l}^{(k,c)},\boldsymbol{x}_{i}) = \frac{p(l|\boldsymbol{x}_{i};\boldsymbol{\Theta}) \pi_{l}^{(k,c)}}{\sum_{l \in \mathcal{L}} p(l|\boldsymbol{x}_{i};\boldsymbol{\Theta}) \pi_{l}^{(k,c)}}. \text{ We define } \\ &\phi(\boldsymbol{\pi},\bar{\boldsymbol{\pi}}) \\ &= -\frac{1}{N} \sum_{i=1}^{N} \sum_{k=1}^{K-1} \sum_{c=1}^{2} d_{i}^{(k,c)} \sum_{l \in \mathcal{L}} \xi_{l}(\bar{\boldsymbol{\pi}}_{l}^{(k,c)},\boldsymbol{x}_{i}) \log \left(\frac{p(l|\boldsymbol{x}_{i};\boldsymbol{\Theta}) \pi_{l}^{(k,c)}}{\xi_{l}(\bar{\boldsymbol{\pi}}_{l}^{(k,c)},\boldsymbol{x}_{i})} \right). \end{split}$$

From Eq. (12) and Eq. (13), we know that $\phi(\pi, \bar{\pi})$ is an upper bound for $\mathcal{R}(\pi, \Theta; \mathcal{S})$, which means that for any π and $\bar{\pi}$, we have $\phi(\pi, \bar{\pi}) \geq \mathcal{R}(\pi, \Theta; \mathcal{S})$, and $\phi(\pi, \pi) = \mathcal{R}(\pi, \Theta; \mathcal{S})$. Assume $\pi^{(t)}$ is a point at the t-th iteration, then $\phi(\pi, \pi^{(t)})$ is an upper bound for $\mathcal{R}(\pi, \Theta; \mathcal{S})$. In the next iteration, there has at least one point $\pi^{(t+1)}$ that satisfies the inequality $\phi(\pi^{(t+1)}, \pi) \leq \mathcal{R}(\pi^{(t)}, \Theta; \mathcal{S})$, which implies $\mathcal{R}(\pi^{(t+1)}, \Theta; \mathcal{S}) \leq \mathcal{R}(\pi^{(t)}, \Theta; \mathcal{S})$, because $\phi(\pi^{(t+1)}, \pi) = \mathcal{R}(\pi^{(t+1)}, \Theta; \mathcal{S})$. Thus, we can minimize $\phi(\pi, \bar{\pi})$ instead of $\mathcal{R}(\pi, \Theta; \mathcal{S})$ after ensuring that $\mathcal{R}(\pi^{(t)}, \Theta; \mathcal{S}) = \phi(\pi^{(t)}, \bar{\pi})$, i.e., $\bar{\pi} = \pi^{(t)}$. Then we have

$$\pi^{(t+1)} = \arg\min_{\pi} \phi(\pi, \pi^{(t)}), \quad s.t., \quad \forall \ l, k, \sum_{c=1}^{2} \pi_{l}^{(k,c)} = 1,$$
(14)

which leads to minimizing the Lagrangian defined by

$$\varphi(\boldsymbol{\pi}, \boldsymbol{\pi}^{(t)}) = \phi(\boldsymbol{\pi}, \boldsymbol{\pi}^{(t)}) + \sum_{k=1}^{K-1} \sum_{l \in \mathcal{L}} \lambda_l^k (\sum_{c=1}^2 \pi_l^{(k,c)} - 1), (15)$$

where λ_l^k is the Lagrange multiplier. By setting $\frac{\partial \varphi(\pi, \pi^{(t)})}{\partial \pi_l^{(k,c)}} = 0$, we have

$$\lambda_{l}^{k} = \frac{1}{N} \sum_{i=1}^{N} \sum_{c=1}^{2} d_{i}^{(k,c)} \xi_{l}(\pi_{l}^{(k,c)(t)}, \boldsymbol{x}_{i}),$$

$$\pi_{l}^{(k,c)(t+1)} = \frac{\sum_{i=1}^{N} d_{i}^{(k,c)} \xi_{l}(\pi_{l}^{(k,c)(t)}, \boldsymbol{x}_{i})}{\sum_{c=1}^{2} \sum_{i=1}^{N} d_{i}^{(k,c)} \xi_{l}(\pi_{l}^{(k,c)(t)}, \boldsymbol{x}_{i})}.$$
(16)

Then the π_l^{k} (t+1) can be updated by:

$$\pi_l^{k\ (t+1)} = \pi_l^{(k,c=1)(t+1)}$$

$$= \frac{\sum_{i=1}^{N} d_{i}^{(k,c=1)} \xi_{l}(\pi_{l}^{(k,c=1)(t)}, \boldsymbol{x}_{i})}{\sum_{i=1}^{N} d_{i}^{(k,c=1)(t)} \xi_{l}(\pi_{l}^{(k,c=1)(t)}, \boldsymbol{x}_{i}) + \sum_{i=1}^{N} d_{i}^{(k,c=2)} \xi_{l}(\pi_{l}^{(k,c=2)(t)}, \boldsymbol{x}_{i})}$$

$$= \frac{\sum_{i=1}^{N} d_{i}^{k} \xi_{l}(\pi_{l}^{k}(t), \boldsymbol{x}_{i})}{\sum_{i=1}^{N} d_{i}^{k} \xi_{l}(\pi_{l}^{k}(t), \boldsymbol{x}_{i}) + \sum_{i=1}^{N} (1 - d_{i}^{k}) \xi_{l}((1 - \pi_{l}^{k}(t)), \boldsymbol{x}_{i})}.$$
(17)

Eq. (17) is the update scheme for the ordinal distributions held by the leaf nodes. The starting point $\pi_l^{(0)}$ can be arbitrary as long as every element is positive, and belongs to [0,1]. In this paper, we initialize π_l^{k} (0) as $\frac{1}{2}$, for $\forall \ l \in \mathcal{L}, k \in \{1,2,\cdots,K-1\}$.

Algorithm 1 The training procedure of a DORFs.

```
    Input: S: training set; n<sub>B</sub>: the number of mini-batches to update π; n<sub>I</sub>: iteration to update π.
    Initialization: Initialize Θ randomly, let π<sub>l</sub><sup>k(0)</sup> = ½ for ∀ l ∈ L, k ∈ {1, 2, ···, K − 1}, and set B = {∅}.
    while Not converge do
    while |B| < n<sub>B</sub> do
    Select a mini-batch B from S randomly
    Update Θ by computing gradient (Eq. (18)) on B
    B = B ∪ B
    end while
    Update π by iterating Eq. (17) on B, and repeat n<sub>I</sub> times
    B = {∅}
    end while
```

F. Learning an Ordinal Regression Forest

As an ensemble of decision trees, we denote a forest as $\mathcal{F} = \{\mathcal{T}_1, \mathcal{T}_2, \cdots, \mathcal{T}_M\}$, where \mathcal{T}_i represents the i-th decision tree. In the training phase, all trees in the forest \mathcal{F} use the same parameters Θ of the feature function $f(\cdot;\Theta)$, but the index function φ of each tree is different and the leaf node ordinal distribution π of each tree is independent. Since a forest is an integration of all trees, the loss function for a forest is given by the averaged loss functions of all trees, i.e., $\mathcal{R}_{\mathcal{F}} = \frac{1}{M} \sum_{m=1}^{M} \mathcal{R}_{\mathcal{T}_m}$, where $\mathcal{R}_{\mathcal{T}_m}$ is the loss function for tree \mathcal{T}_m defined in Eq. (4). Obviously, learning a forest also requires to estimate the parameters Θ of the split node and the leaf node ordinal distributions π of each tree. According to the alternative optimization strategy, we learn Θ by fixing the leaf node ordinal distribution π of all the trees in the forest \mathcal{F} . Based on the derivation in Sec. III-C, we have

$$\frac{\partial \mathcal{R}_{\mathcal{F}}}{\partial \mathbf{\Theta}} = \frac{1}{M} \sum_{i=1}^{N} \sum_{m=1}^{M} \sum_{n \in \mathcal{N}_m} \frac{\partial \mathcal{R}_{\mathcal{T}_m}}{\partial f_{\varphi_{m(n)}}(\mathbf{x}_i; \mathbf{\Theta})} \frac{\partial f_{\varphi_{m(n)}}(\mathbf{x}_i; \mathbf{\Theta})}{\partial \mathbf{\Theta}},$$
(18)

where $\varphi_m(\cdot)$ and \mathcal{N}_m are the index function and the split node set of the m-th tree \mathcal{T}_m , respectively. We know that the index function $\varphi_m(\cdot)$ of each tree is initialized randomly before tree learning, so that the split nodes correspond to a subset of output units of f. This strategy increases the randomness in training to reduce the risk of overfitting.

Since each tree in the forest \mathcal{F} has its own leaf node ordinal distribution π , we can update them independently by Eq. (17) when Θ is fixed. For implementation convenience, the leaf node ordinal distributions π are updated on a set of minibatches \mathcal{B} rather than on the whole dataset \mathcal{S} . The training procedure of a DORFs is shown in Algorithm 1.

In the process of testing, the output of a forest is the average output of all the individual trees, as follows:

$$g(x; \Theta, \mathcal{F}) = \frac{1}{M} \sum_{m=1}^{M} g(x; \Theta, \mathcal{T}_m)$$
 (19)

IV. EXPERIMENTS

To demonstrate the effectiveness of DORFs, we verify it on two typical ordinal regression tasks, *i.e.*, facial age estimation and image aesthetic assessment.



Fig. 3. Some facial image samples from three age estimation databases, including (a) FGNET, (b) MORPH, (c) CACD.

A. Data Preparation

In our experiments, we train and evaluate our method on three facial age estimation datasets: FGNET [43], MORPH [44], and the Cross-Age Celebrity Dataset (CACD) [45]; and two image aesthetic assessment datasets: Aesthetics Visual Analysis dataset (AVA) [46] and Aesthetics and Attributes database (AADB) [13].

FGNET is a database used for age estimation, which consists of only 1,002 color or gray facial images of 82 subjects with large variations in pose, expression, and lighting. For each subject, there are more than ten images ranging from age 0 to age 69. MORPH is one of the most popular facial age estimation dataset, which contains 55,134 facial images of 13,617 subjects ranging from 16 to 77 years old. CACD is another largest facial age estimation database, which contains around 160,000 facial images of 2,000 celebrities. All facial images are aligned by the five facial landmarks detected by MTCNN [47]. Following [48], we use the leave-one-personout (LOPO) protocol in the FGNET dataset and employ the five-fold random split (RS) protocol and the five-fold subjectexclusive (SE) protocol in MORPH dataset. According to [27], CACD is divided into three subsets: the training set composed of 1,800 celebrities, the testing set that has 120 celebrities and the validation set containing 80 celebrities. The partitioning interval η is set as 1 in three facial age estimation databases.

AVA is the largest image aesthetics assessment dataset and contains more than 250,000 pictures that are downloaded from well-known photographer community sites named *dpchallenge*. The aesthetic quality of each image is rated by a score vector which ranges from 1 to 10. In our task, we average the score vector and convert the average score into an ordinal distribution with a partitioning interval of 0.1. Followed by [46], we adopt the same setting to split the dataset. **AADB** is another common image aesthetics assessment dataset. Different from the AVA dataset, AADB contains 10,000 pictures labeled by scalars representing their average aesthetic score collected from *flickr* with the score ranges from 0 to 1 and all pictures are the natural images without artificial modification. In this work, the 9,000 of 10,000 pictures are

used for training and the rest are for testing. The partitioning interval is set as 0.05 in the AADB dataset.

Before fed into the networks, all the input images are randomly cropped into $256 \times 256 \times 3$ and then resized into $224 \times 224 \times 3$. In order to better understand these dataset, we show some facial age estimation samples and some aesthetic assessment samples in Fig. 3 and Fig. 4, respectively.

B. Implementation Details

Since the DORFs is modular and its feature function can be implemented as a standard neural network layer, we can integrate it with any deep networks. Following the recent CNN-based methods [27], [48], [49], we use the VGG-16 that is pre-trained with ImageNet [50] as the backbone of our method. The default settings for the parameters of our method are: number of trees (5), tree depth (6), number of output units in the feature learning function (128), number of iterations to update leaf node predictions (20), number of mini-batches used to update leaf node predictions (10). The network training based hyper-parameters are: initial learning rate (0.001), mini-batch size (64), maximal epochs (40), and the probability of dropout is 0.5. We decrease the learning rate $(\times 0.2)$ every 15 epochs. To further validate the effectiveness of the DORFs, we implement a deep ordinal regression (DOR) method as a baseline. DOR utilizes VGG-16 as its backbone and the output layer is the same as the OR-CNN [10].

C. Evaluation on Facial Age Estimation

We evaluate the DORFs on three public facial age estimation datasets, *i.e.*, FGNET, MORPH, and CACD, and compare it with several ordinal regression methods (*e.g.*, OHRank [51], OR-CNN [10], and Ranking-CNN [11]) and the state-of-theart methods of age estimation (*e.g.*, Mean-Variance [48] and DRFs [27]). Further, we evaluate the performance of age estimation by two measurements, *i.e.*, Mean Absolute Error (MAE) and the Cumulative Score (CS).

The results of DORFs and the competitors are summarized in Table I. It can be seen that DORFs outperforms three state-of-the-art ordinal regression methods (OHRank, OR-CNN,

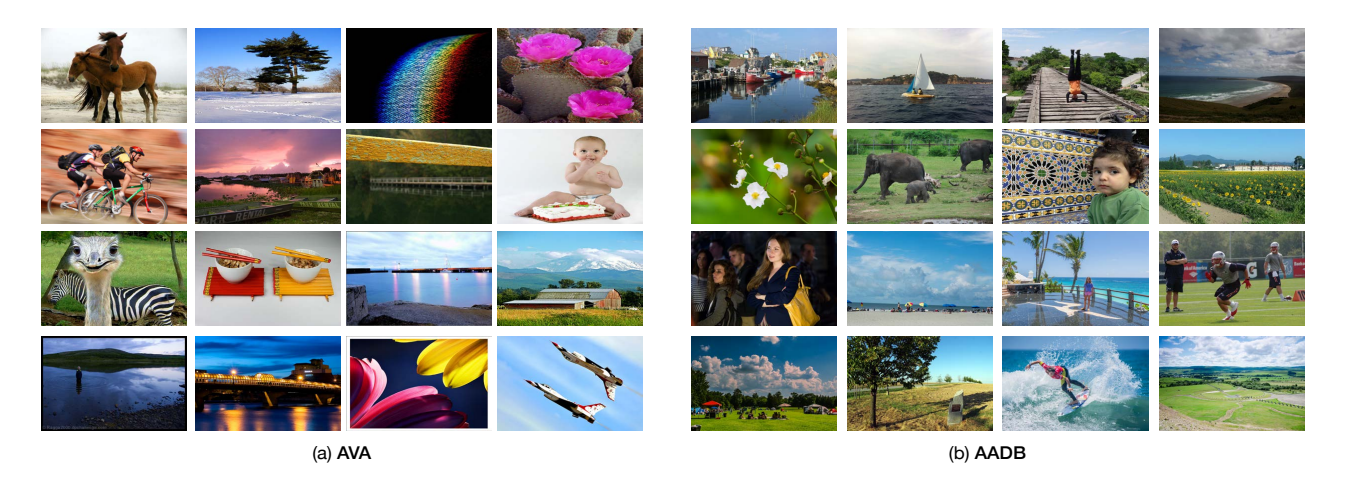


Fig. 4. Some aesthetic assessment samples from the AVA and the AADB datasets.

TABLE I

PERFORMANCE COMPARISONS BETWEEN THE DORFS AND THE STATE-OF-THE-ARTS ON THE FGNET, MORPH, AND CACD DATASETS. (THE BOLD VALUES DENOTE THE BEST PERFORMANCE, AND THE UNDERLINED VALUES INDICATE THE SECOND BEST PERFORMANCE.)

Dataset	Evaluation	OHRank [51]	OR-CNN [10]	Ranking-CNN [11]	Mean-Variance [48]	DRFs [27]	DORFs (Ours)
FGNET	MAE	4.48	N/A	N/A	4.10	3.85	2.68
FUNEI	CS(L=5)	74.4%	N/A	N/A	78.2%	80.6%	86.80%
MORPH	MAE	3.82	3.27	2.96	2.41	2.17	2.19
MOKFII	CS(L=5)	N/A	73.0%	85.0%	90.0%	91.3%	93.0%
CACD	MAE(train)	N/A	4.89	N/A	4.64	4.64	4.67
CACD	MAE(val)	N/A	6.87	N/A	6.29	5.77	<u>6.10</u>

and Ranking-CNN) and achieves a comparable performance with two state-of-the-art age estimation methods (Mean-Variance and DRFs) on the facial age estimation datasets. This result can verify the effectiveness and superiority of the proposed method over the existing ordinal regression methods to a certain extent. It is worth noting that our DORFs achieve significant performance refinement compared with other methods on the FGNET dataset, which is the smallest age estimation dataset among three benchmark datasets. It indicates that our method is more stable and has a better generalization performance in the small dataset.

To further verify the effectiveness of DORFs, we compare it with DOR on FGNET and MORPH datasets. In order to eliminate the impact of network parameters and network size on performance, both DOR and DORFs utilize VGG-16 as their backbone. From Table II, we learn that DORFs performs better than DOR in all situations. It demonstrates that learning a global ordinal distribution can obtain better predictive performance than learning a series of binary classifiers independently.

Moreover, we can see that DOR is more prone to overfitting than DORFs on cross-entropy loss (see Fig. 5 (a)), which means DORFs is more stable. Note that the over-fitting issue of DOR is less obvious in MAE loss (see Fig. 5 (b)), because the calculation manner of MAE (see Eq. (1)) may have some fault tolerance. In conclusion, DORFs is more effective and stable than DOR, because learning an ordinal distribution can better preserve the global ordinal relationship among these binary classifiers and combining with an ensemble method,

i.e., decision tree, make our model more stable.

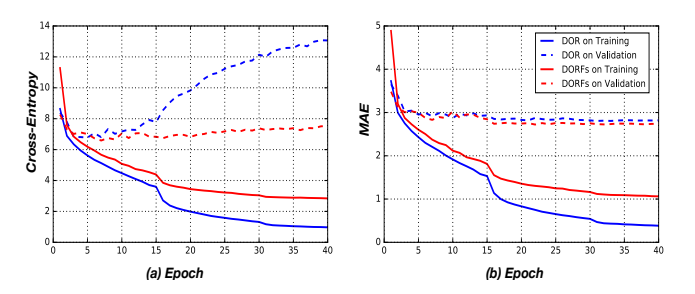


Fig. 5. The train and validation losses on MORPH (SE), *i.e.*, (a) cross-entropy loss and (b) MAE loss.

D. Evaluation on Image Aesthetic Assessment

We validate our DORFs on two image aesthetics assessment datasets, *i.e.*, AVA and AADB, by comparing with the state-of-the-art aesthetics assessment methods and several ordinal regression methods. Further, Pearson Linear Correlation Coefficient (PLCC) and Spearmans Rank Correlation Coefficient (SRCC) are computed between the predicted and ground truth aesthetics mean scores for measuring the correlation-based performance of image aesthetics assessment. We know that the PLCC is a statistic that measures linear correlation between two variables and it has a value between 1 and -1, where 1 is total positive linear correlation, 0 is no linear correlation, and -1 is total negative linear correlation. Similar to the PLCC,

	FGNET		MORPH				
Method	LOPO		RS		SE		
	MAE	CS (L = 5)	MAE	CS (L = 5)	MAE	CS $(L = 5)$	
DOR	3.49	80.87%	2.30	91.60%	2.77	87.50%	
DODE: (Oure)	2.68	86 80 %	2 10	03 00%	2.60	80 UU 0/2	

TABLE II

COMPARISONS BETWEEN DOR AND DORFS IN TERMS OF MAE AND CS.

the SRCC can be defined as the Pearson correlation coefficient between two rank variables.

From the results of Table III, it can be seen that DORFs outperforms the current image aesthetics assessment methods and other ordinal regression methods on AADB dataset. Besides, our method achieves a comparable performance on AVA dataset. The GPF-CNN outperforms our method, but it is more complicated both in data processing and backbone network. To sum up, the proposed method is effective on image aesthetic assessment.

E. Discussion

Parameters: Number of Tree and Tree Depth As an ensemble model, the proposed DORFs has two important hyper-parameters: number of tree and tree depth. Now we change each of them and fix the other one to the default value (number of tree (5) and tree depth (6)) to see how the performance changes on MORPH (SE). As shown in Fig. 6 (a), the more trees we have, the better performance the DORFs will have. Besides, with the tree depth increase, as shown in Fig. 6 (b), the MAE first starts to decrease and then becomes stable.

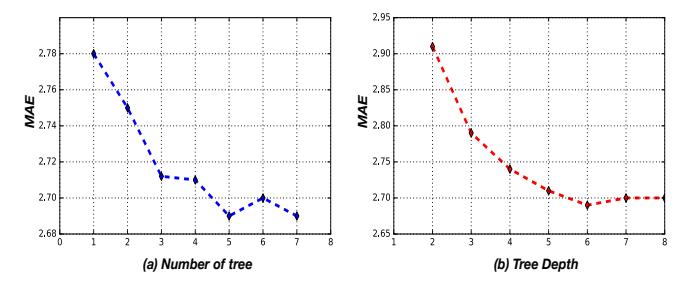


Fig. 6. The performance changes by varying (a) number of tree and (b) tree depth on MORPH (SE).

Visualization of the Leaf Nodes To better understand the DORFs, we visualize the output of leaf nodes learned on MORPH. We can see that different leaf node learns different ordinal distribution, e.g., leaf node from Fig. 7 (a) to (d) learns an age distribution of juvenile, youth, middle-aged, and old age, respectively. The distribution diversity of leaf nodes is necessary to model any desired ordinal distribution by a mixture of leaf nodes. According to the update rule of the leaf node (seen in Eq. (17)), the update of leaf node distribution is a weighted combination of the training sample labels. Since the labels of the training sample are all in descending order, e.g., the label 5 years old can be transformed into an ordinal distribution label $[1,1,1,1,0,...,0]^T$ with descending order. Thus the distribution of the leaf node can also preserve the descending order after the weighted combination.

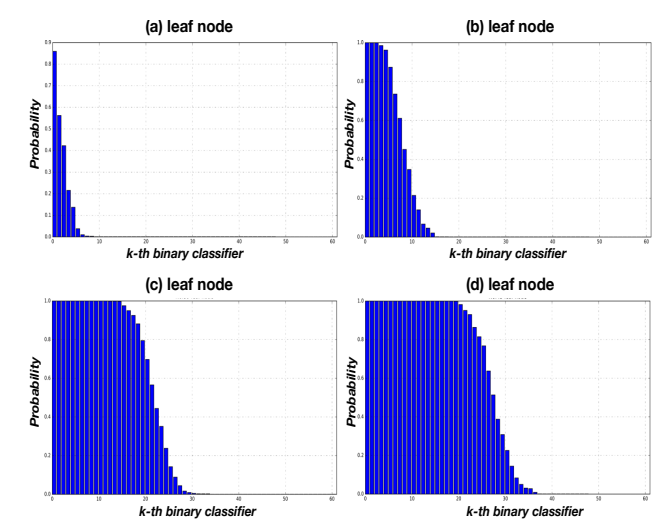


Fig. 7. The visualization of leaf nodes. These nodes from (a) to (d) represent the age distributions of juvenile, youth, middle-aged, and old age, respectively.

Time Complexity The complexity of our model can be analyzed in two separate parts: feature function and the random forests. When using VGG-16 as the backbone, the computational complexity of the feature function is about 15.3G FLOPs. Let H and C denote the tree depth and the dimension of leaf node, respectively. Then each tree contains $D=2^{(H-1)}-1$ split nodes and $2^{(H-1)}$ leaf nodes. The complexity of testing a tree is $\mathcal{O}(D\times C)$. On the MORPH dataset (43,965 training images, 11,100 testing images), our DORFs model only takes 6,680s for training (27000 iterations) and 17s for testing all 11100 images, which highlights that our method only takes 1.5ms to process one image. Therefore, our approach can be used in many real-time prediction scenarios.

F. The Examples Predicted by our DORFs

Fig. 8 and Fig. 9 show some examples of good and poor results by our approach (DORFs) on facial age estimation task (MORPH [44]) and image aesthetic assessment (AADB [13]) task, respectively. We can see that the proposed approach performs well by estimated the ordinal distribution on age estimation and aesthetic assessment (see the top green boxes of Fig. 8 and Fig. 9). However, the age estimation accuracy may decrease for the old people because the distribution of the MOPRH II dataset is pretty imbalanced and the sample of the old man is pretty small (see the bottom red box of Fig. 8). Besides, the aesthetic assessment accuracy may decrease if the images are blurring (see the bottom red box of Fig. 9).

TABLE III

PERFORMANCE COMPARISONS BETWEEN THE PROPOSED DORFS AND THE STATE-OF-THE-ART METHODS ON THE AADB AND THE AVA DATASETS. (THE BOLD VALUES DENOTE THE BEST PERFORMANCE, AND THE UNDERLINED VALUES INDICATE THE SECOND BEST PERFORMANCE.)

Dataset	Evaluation	Reg+Rank [13]	EMD [52]	NIMA-V1 [53]	GPF-CNN [54]	OR-CNN [10]	DOR	DORFs (Ours)
AADB	PLCC	N/A	N/A	N/A	N/A	0.4388	0.6555	0.6829
AADB	SRCC	0.6308	0.6647	N/A	N/A	0.437	0.6416	0.6770
AVA	PLCC	N/A	N/A	0.610	0.6868	0.5076	0.6218	0.6649
AVA	SRCC	0.5126	N/A	0.592	0.6762	0.4986	0.6115	<u>0.6714</u>

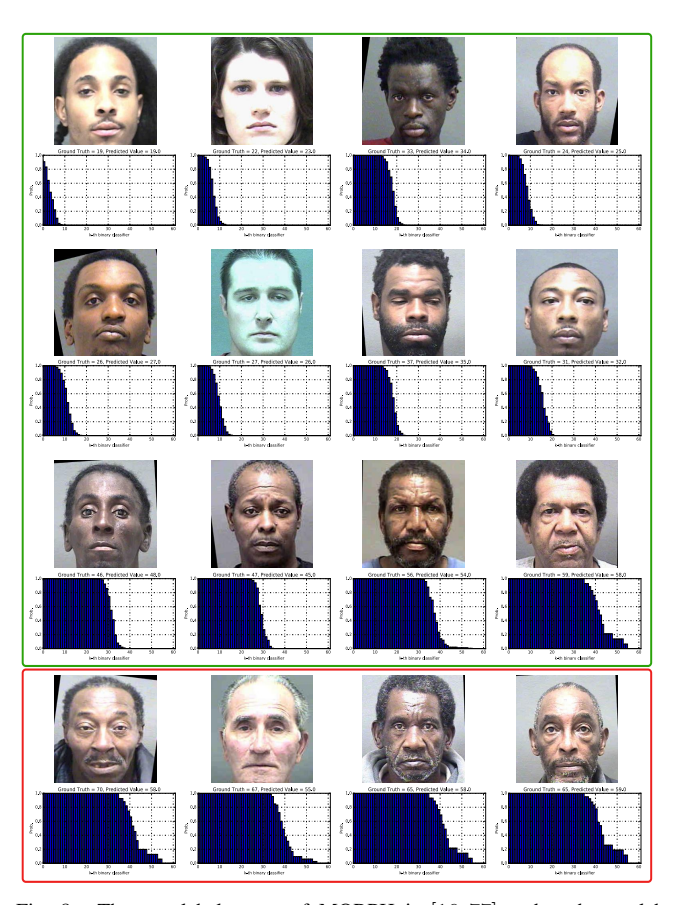


Fig. 8. The age label range of MORPH is [16,77] and each age label is transformed into a 61 dimensionality ordinal distribution label with a partitioning interval 1.

V. CONCLUSION

In this paper, we proposed a deep ordinal regression forests (DORFs) to solve the ordinal regression problem by extending the differentiable decision tree to learn an ordinal distribution, which can better preserve the global ordinal relationship and makes our model both more stable and accurate. Note that it is the first work to obtain ordering results for ordinal regression with the differentiable decision tree. The proposed method overcomes many stability issues of methods solving a series of binary classifiers independently. As a bonus, feature representation can be learned jointly with decision forests in an end-to-end manner. Besides, we provide a theoretical derivation for the update rule of the leaf node. Finally, the experimental results on facial age estimation and image aesthetic assessment tasks demonstrate the effectiveness and

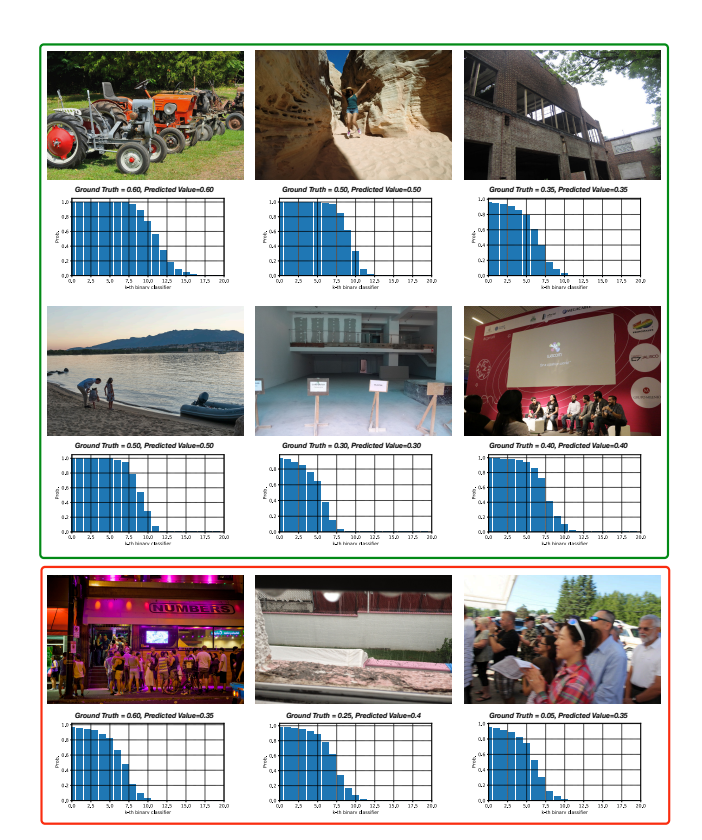


Fig. 9. The label range of AADB is [0,1] and each label is transformed into a 20 dimensionality ordinal distribution label with a partitioning interval 0.05

stability of the DORFs model.

In the future, we will consider extending our ordinal regression framework into other non-image ordinal regression problems, such as credit rating, medical research, and text classification.

REFERENCES

- [1] R. Bender and U. Grouven, "Ordinal logistic regression in medical research," *Journal of the Royal College of physicians of London*, vol. 31, no. 5, p. 546, 1997.
- [2] O. M. Doyle, E. Westman, A. F. Marquand, P. Mecocci, B. Vellas, M. Tsolaki, I. Kłoszewska, H. Soininen, S. Lovestone, S. C. Williams, et al., "Predicting progression of alzheimer's disease using ordinal regression," PloS one, vol. 9, no. 8, 2014.
- [3] M. Pérez-Ortiz, P. A. Gutiérrez, C. García-Alonso, L. Salvador-Carulla, J. A. Salinas-Perez, and C. Hervás-Martínez, "Ordinal classification of depression spatial hot-spots of prevalence," in *IEEE International Conference on Intelligent Systems Design and Applications*, pp. 1170– 1175, 2011.

- [4] J. S. Cardoso, J. F. P. da Costa, and M. J. Cardoso, "Modelling ordinal relations with syms: An application to objective aesthetic evaluation of breast cancer conservative treatment," *Neural Networks*, vol. 18, no. 5-6, pp. 808–817, 2005.
- [5] M. Pérez-Ortiz, M. Cruz-Ramírez, M. D. Ayllón-Terán, N. Heaton, R. Ciria, and C. Hervás-Martínez, "An organ allocation system for liver transplantation based on ordinal regression," *Applied Soft Computing*, vol. 14, pp. 88–98, 2014.
- [6] Y. S. Kwon, I. Han, and K. C. Lee, "Ordinal pairwise partitioning (opp) approach to neural networks training in bond rating," *Intelligent Systems in Accounting, Finance and Management*, vol. 6, no. 1, pp. 23–40, 1997.
- [7] K.-j. Kim and H. Ahn, "A corporate credit rating model using multiclass support vector machines with an ordinal pairwise partitioning approach," *Computers & Operations Research*, vol. 39, no. 8, pp. 1800– 1811, 2012.
- [8] H. Dikkers and L. Rothkrantz, "Support vector machines in ordinal classification: An application to corporate credit scoring," *Neural Network World*, vol. 15, no. 6, p. 491, 2005.
- [9] F. Fernandez-Navarro, P. Campoy-Munoz, C. Hervás-Martínez, X. Yao, et al., "Addressing the eu sovereign ratings using an ordinal regression approach," *IEEE Transactions on Cybernetics*, vol. 43, no. 6, pp. 2228– 2240, 2013.
- [10] Z. Niu, M. Zhou, L. Wang, X. Gao, and G. Hua, "Ordinal regression with multiple output CNN for age estimation," in *IEEE Conference on Computer Vision and Pattern Recognition*, pp. 4920–4928, 2016.
- [11] S. Chen, C. Zhang, M. Dong, J. Le, and M. Rao, "Using ranking-CNN for age estimation," in *IEEE Conference on Computer Vision and Pattern Recognition*, 2017.
- [12] W. Luo, X. Wang, and X. Tang, "Content-based photo quality assessment," in *International Conference on Computer Vision*, pp. 2206–2213, 2011.
- [13] S. Kong, X. Shen, Z. Lin, R. Mech, and C. Fowlkes, "Photo aesthetics ranking network with attributes and content adaptation," in *European Conference on Computer Vision*, pp. 662–679, Springer, 2016.
- [14] S. Baccianella, A. Esuli, and F. Sebastiani, "Feature selection for ordinal text classification," *Neural Computation*, vol. 26, no. 3, pp. 557–591, 2014
- [15] F. E. Harrell Jr, Regression modeling strategies: With applications to linear models, logistic and ordinal regression, and survival analysis. Springer-Verlag New York, 2001.
- [16] R. Herbrich, T. Graepel, and K. Obermayer, "Support vector learning for ordinal regression," *International Conference on Artificial Neural* Networks, pp. 97–102, 1999.
- [17] A. Shashua and A. Levin, "Ranking with large margin principle: two approaches," in *International Conference on Neural Information Processing Systems*, pp. 961–968, 2003.
- [18] K. Crammer and Y. Singer, "Pranking with ranking," in *International Conference on Neural Information Processing Systems*, pp. 641–647, 2002
- [19] W. Chu and S. S. Keerthi, "Support vector ordinal regression," *Neural computation*, vol. 19, no. 3, pp. 792–815, 2007.
- [20] H.-T. Lin and L. Li, "Large-margin thresholded ensembles for ordinal regression: Theory and practice," in *International Conference on Algorithmic Learning Theory*, pp. 319–333, Springer, 2006.
- [21] A. Riccardi, F. Fernandez-Navarro, and S. Carloni, "Cost-sensitive adaboost algorithm for ordinal regression based on extreme learning machine," *IEEE Transactions on Cybernetics*, vol. 44, no. 10, pp. 1898– 1909, 2014.
- [22] M. Perez-Ortiz, P. Gutierrez, and C. Hervas-Martinez, "Projection-based ensemble learning for ordinal regression," *IEEE Transactions on Cybernetics*, vol. 44, no. 5, pp. 681–694, 2014.
- [23] E. Frank and M. Hall, "A simple approach to ordinal classification," in *European Conference on Machine Learning*, pp. 145–156, 2001.
- [24] H.-T. Lin and L. Li, "Reduction from cost-sensitive ordinal ranking to weighted binary classification," *Neural Computation*, vol. 24, no. 5, pp. 1329–1367, 2012.
- [25] H. Fu, M. Gong, C. Wang, K. Batmanghelich, and D. Tao, "Deep ordinal regression network for monocular depth estimation," in *IEEE Conference on Computer Vision and Pattern Recognition*, pp. 2002–2011, 2018.
- [26] P. Kontschieder, M. Fiterau, A. Criminisi, and S. Rota Bulo, "Deep neural decision forests," in *International Conference on Computer Vision*, pp. 1467–1475, 2015.
- [27] W. Shen, Y. Guo, Y. Wang, K. Zhao, B. Wang, and A. L. Yuille, "Deep regression forests for age estimation," in *IEEE Conference on Computer Vision and Pattern Recognition*, pp. 2304–2313, 2018.

- [28] M. I. Jordan, Z. Ghahramani, T. S. Jaakkola, and L. K. Saul, "An introduction to variational methods for graphical models," *Machine Learning*, vol. 37, no. 2, pp. 183–233, 1999.
- [29] A. L. Yuille and A. Rangarajan, "The concave-convex procedure," Neural Computation, vol. 15, no. 4, pp. 915–936, 2003.
- [30] Y. Amit and D. Geman, "Shape quantization and recognition with randomized trees," *Neural Computation*, vol. 9, no. 7, pp. 1545–1588, 1997
- [31] L. Breiman, "Random forests," *Machine Learning*, vol. 45, no. 1, pp. 5–32, 2001.
- [32] A. Criminisi and J. Shotton, Decision forests for computer vision and medical image analysis. Springer Science & Business Media, 2013.
- [33] T. K. Ho, "Random decision forests," in *International Conference on Document Analysis and Recognition*, vol. 1, pp. 278–282, 1995.
- [34] M. I. Jordan and R. A. Jacobs, "Hierarchical mixtures of experts and the em algorithm," *Neural Computation*, vol. 6, no. 2, pp. 181–214, 1994
- [35] C. M. Bishop and M. Svenskn, "Bayesian hierarchical mixtures of experts," in *Artificial Intelligence*, pp. 57–64, Morgan Kaufmann Publishers Inc., 2002.
- [36] W. Shen, K. Zhao, Y. Guo, and A. L. Yuille, "Label distribution learning forests," in *International Conference on Neural Information Processing* Systems, pp. 834–843, 2017.
- [37] A. Roy and S. Todorovic, "Monocular depth estimation using neural regression forest," in *IEEE Conference on Computer Vision and Pattern Recognition*, pp. 5506–5514, 2016.
- [38] J. Albert and S. Chib, "Bayesian methods for cumulative, sequential and two-step ordinal data regression models," Report. Department of Mathematics and Statistics, Bowling Green State University, 1997.
- [39] W. Chu and Z. Ghahramani, "Gaussian processes for ordinal regression," *Journal of Machine Learning Research*, vol. 6, no. Jul, pp. 1019–1041, 2005.
- [40] K. Dembczyński, W. Kotłowski, and R. Słowiński, "Ordinal classification with decision rules," in *International Workshop on Mining Complex Data*, pp. 169–181, Springer, 2007.
- [41] A. Agresti, Analysis of ordinal categorical data, vol. 656. John Wiley & Sons, 2010.
- [42] L. Li and H.-T. Lin, "Ordinal regression by extended binary classification," in *International Conference on Neural Information Processing* Systems, pp. 865–872, 2007.
- [43] G. Panis, A. Lanitis, N. Tsapatsoulis, and T. F. Cootes, "Overview of research on facial ageing using the FG-NET ageing database," *Biometrics*, vol. 5, no. 2, pp. 37–46, 2016.
- [44] K. Ricanek and T. Tesafaye, "Morph: A longitudinal image database of normal adult age-progression," in Automatic Face and Gesture Recognition, pp. 341–345, 2006.
- [45] B.-C. Chen, C.-S. Chen, and W. H. Hsu, "Face recognition and retrieval using cross-age reference coding with cross-age celebrity dataset," *IEEE Transactions on Multimedia*, vol. 17, no. 6, pp. 804–815, 2015.
- [46] N. Murray, L. Marchesotti, and F. Perronnin, "AVA: A large-scale database for aesthetic visual analysis," in *IEEE Conference on Computer Vision and Pattern Recognition*, pp. 2408–2415, 2012.
- [47] K. Zhang, Z. Zhang, Z. Li, and Y. Qiao, "Joint face detection and alignment using multitask cascaded convolutional networks," *IEEE Signal Processing Letters*, vol. 23, no. 10, pp. 1499–1503, 2016.
- [48] H. Pan, H. Han, S. Shan, and X. Chen, "Mean-variance loss for deep age estimation from a face," in *IEEE Conference on Computer Vision* and Pattern Recognition, pp. 5285–5294, 2018.
- [49] R. Rothe, R. Timofte, and L. Van Gool, "Deep expectation of real and apparent age from a single image without facial landmarks," *International Journal of Computer Vision*, vol. 126, no. 2-4, pp. 144– 157, 2018.
- [50] O. Russakovsky, J. Deng, H. Su, J. Krause, S. Satheesh, S. Ma, Z. Huang, A. Karpathy, A. Khosla, M. Bernstein, et al., "Imagenet large scale visual recognition challenge," *International Journal of Computer Vision*, vol. 115, no. 3, pp. 211–252, 2015.
- [51] K.-Y. Chang, C.-S. Chen, and Y.-P. Hung, "Ordinal hyperplanes ranker with cost sensitivities for age estimation," in *IEEE Conference on Computer Vision and Pattern Recognition*, pp. 585–592, 2011.
- [52] L. Hou, C.-P. Yu, and D. Samaras, "Squared earth mover's distance-based loss for training deep neural networks," arXiv:1611.05916, 2016.
- [53] H. Talebi and P. Milanfar, "NIMA: Neural image assessment," IEEE Transactions on Image Processing, vol. 27, no. 8, pp. 3998–4011, 2018.
- [54] X. Zhang, X. Gao, W. Lu, and L. He, "A gated peripheral-foveal convolutional neural network for unified image aesthetic prediction," *IEEE Transactions on Multimedia*, vol. 21, no. 11, pp. 2815–2826, 2019.